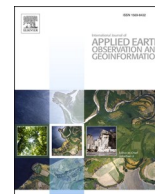


Contents lists available at [ScienceDirect](https://www.sciencedirect.com)

International Journal of Applied Earth Observation and Geoinformation

journal homepage: www.elsevier.com/locate/jag

Division of the tropical savanna fire season into early and late dry season burning using MODIS active fires

Tom Eames^{a,*}, Roland Vernooij^c, Jeremy Russell-Smith^b, Cameron Yates^b, Andrew Edwards^b, Guido R. van der Werf^c

^a Department of Earth Sciences, Faculty of Science, Vrije Universiteit Amsterdam, Amsterdam, The Netherlands

^b Research Institute for the Environment and Livelihoods, Charles Darwin University, Casuarina, Darwin, Northern Territory, Australia

^c Meteorology and Air Quality Section, Wageningen University & Research, Wageningen, The Netherlands

ARTICLE INFO

Keywords:

Fire
Fire management
Remote sensing
Earth observation
MODIS
Active fires
Tropical savanna
Fire seasonality
Biomass burning

ABSTRACT

Tropical savannas and grasslands are the most frequently burned biome in the world, and fire has an important role in sustaining ecosystem processes. Modern management of fires in savannas has roots in traditions stretching back centuries, and nowadays earth observation data is incorporated extensively in fire management practices. In tropical savannas in particular strongly seasonal monsoonal climates allow relatively low severity prescribed burning in the early part of the dry season (EDS) with the goal of preventing more destructive late dry season (LDS) fires. In many regional contexts it is common that a specific, fixed date is used officially to indicate when the window of safe burning has expired and the EDS transitions to the LDS, based on the experience of local or regional fire management authorities. This approach, while practical, neglects inter-annual variability in meteorological conditions and timing of onset of more dangerous fire weather. In this study, we propose a remote sensing-based method for determining when this EDS window expires for five savanna-dominated continental-scale regions. By taking advantage of the fact that conditions allowing night-time burning occur later in the dry season, we use day and night-time active fire detections from the MODerate Resolution Imaging Spectroradiometer (MODIS) instruments to set a flexible date of transition between the EDS and LDS. The vast majority of tropical savannas have very variable (std. dev. \approx 20–40 days) transition dates, though this is somewhat modulated by fire frequency. Fuel connectivity rather than fuel condition appears to be a strong driving factor behind this variability. We find that especially national parks and protected areas have a high proportion of potentially more severe burning in the LDS, though areas with well-established EDS burning programmes are reducing this impact.

1. Introduction

Tropical savannas are the world's most burned biome, accounting for more than two thirds of global burned area annually (Werf et al., 2017; Giglio et al., 2013). Fires in these regions occur typically frequently, with average return times of a few years and some areas even experiencing annual burning. Much of the flora is adapted to such a frequent fire regime through e.g. thicker bark, raised canopies, fast resprouting or seeds which germinate when exposed to fire (Groom and Lamont, 2015; Chief et al., 1987; Simon and Pennington, 2012). Disturbance from fire plays a key role in sustaining ecological function, dynamic processes, and biodiversity in savanna ecosystems (Scholes and Walker, 1993; Scholes and Archer, 1997; Sankaran et al., 2005). Fire-related processes

are argued to have been a driving force in the creation of savannas worldwide (Beerling and Osborne, 2006).

Tropical savanna regions generally have two distinct seasons in a year, a 4–6 month wet season where most or all of the rainfall in any given year occurs, and a dry season in which very little or no rainfall occurs (Archibald et al., 2019). Fires in tropical savannas occur predominantly during the dry season. Fires occurring throughout the early dry season (EDS) period tend to be less extensive, spatially more patchy, and of lower severity than fires occurring later in the season under more severe fire weather (higher temperatures, lower humidity, often more windy) and fully cured fuel conditions (Williams et al., 2003; Gambiza et al., 2005; Perry et al., 2019). These contrasting seasonal conditions have long been exploited by communities across savanna-dominated

* Corresponding author.

E-mail address: t.c.eames@vu.nl (T. Eames).

<https://doi.org/10.1016/j.jag.2023.103575>

Received 13 July 2023; Received in revised form 9 November 2023; Accepted 16 November 2023

Available online 22 November 2023

1569-8432/© 2023 The Authors. Published by Elsevier B.V. This is an open access article under the CC BY license (<http://creativecommons.org/licenses/by/4.0/>).

Table 1

Proportion of global tropical savanna (Olson et al., 2001) and global burned area from MCD64A1 C6.1 (Werf et al., 2017) for the 5 tropical savanna zones.

core region	Tropical savanna	Burned area
Northern hemisphere South America (NHSA)	2.2 %	0.7 %
Southern hemisphere South America (SHSA)	18.0 %	3.3 %
Northern hemisphere Africa (NHAF)	33.5 %	28.2 %
Southern hemisphere Africa (SHAF)	27.5 %	30.2 %
Australia (AUST)	10.3 %	6.8 %
Global	91.5 %	69.2 %

regions for purposes including but not limited to hunting/gathering (Eriksen, 2007; Hill et al., 1999; Hough, 1993; Pivello, 2011); subsistence agriculture (Butz, 2009; Eriksen, 2007); biodiversity management (Eriksen, 2007; Laris, 2002; Pivello, 2011); land regeneration (Hill et al., 1999; Mistry et al., 2005); reducing the risk of undesirable fires (Huffman, 2013; Butz, 2009; Eriksen, 2007; Laris, 2002; Pivello, 2011) and, more recently, carbon emissions and offsetting activities (Russell-Smith et al., 2013; Fitzsimons et al., 2012).

For many fire and land management applications it is crucial to understand how the fire seasonal conditions progress in respective savanna regions. For reducing LDS wildfire risks, prescribed fire management practices are typically undertaken in the EDS under milder fire weather and fuel conditions (Perry et al., 2019; Laris, 2002; Eriksen, 2007; Butz, 2009; Mistry et al., 2005). This is particularly important in savannas with a low human footprint, such as protected areas like national parks. Restrictions on building and development mean that these areas usually are sparsely populated, possess minimal infrastructure, urbanisation, or other geographical features which could act as a barrier for wildfire spread (Archibald et al., 2010). In the absence of such barriers, wildfires can spread more extensively in these areas. This can be exacerbated when the fire season transitions from EDS to LDS and fires are increasingly likely to persist overnight. Active management to combat these often more destructive and undesirable LDS fires is especially necessary in these protected areas.

In most savanna regions the EDS to LDS transition is defined formally by an invariant annually fixed date (e.g. end of June in parts of southern Africa (Russell-Smith et al., 2021; Archibald et al., 2009); start of December in Mali (Laris, 2002); end of July in Northern Australia (Perry et al., 2020); end of June in Brazil (Barradas et al., 2018)). Although backed by extensive institutional and traditional knowledge experience (e.g. in Australia (Garde et al., 2009; Russell-Smith et al., 2003)) such fixed protocols do not allow for considerable inter-annual and inter-regional variability with potentially significant implications. Fire management protocols, including prescribed burning, can be costly to plan and execute. With a more certain time frame to the fire season costs to areas already on a restricted budget such as protected areas or national parks may be reduced in the EDS. Furthermore, if the start of the LDS is well defined then the onset of conditions conducive to more destructive burning (Williams et al., 2003; Gambiza et al., 2005; Perry et al., 2019) can be anticipated and prepared for more effectively. Additionally, the constraining of the EDS/LDS transition date may reduce the impact of possible erroneous accounting of seasonal emissions from savanna fire management projects (Perry et al., 2020).

Remote sensing and earth observation (EO) data have been used to monitor fire activity in a host of different ways, from defining and calculating burned area (Giglio et al., 2013; Giglio et al., 2018; M. P. Martin et al., 2006); assessing fire severity (Edwards et al., 2013; Gibson et al., 2020) to analysis of fire regimes/behaviour (Archibald et al., 2009; Andela et al., 2019; Price et al., 2012; Archibald et al., 2010). Recently the focus has been on improving the detection of smaller fires with higher resolution data, as EO data with coarse resolution cannot detect these small but ubiquitous fires (Ramo et al., 2021). Often burned area data is augmented by active fire detections such as those from MODIS (Giglio et al., 2016). These are datapoints where even small fires occurring some- where within a pixel can be detected (Giglio et al.,

2006), and have been used to augment lower resolution burned area data to allow for the inclusion of small fires (Werf et al., 2017).

In the following paper we make use of active fire detections as a proxy for fire activity. We aim to provide a new method for defining the EDS to LDS transition date based on assessment of seasonal changes in day-time to night-time active fire hotspots derived from the MODIS archive, 2003–2021. Making use of these transition dates, we then split burned area into EDS and LDS activity in several key core regions comprising 92 % of the distribution of tropical savannas and almost 70 % of global fire extent. Using a random forest decision tree, we investigated to what extent meteorological conditions drive variability in the transition date. We were also able to identify regions which have a fire regime skewed towards the LDS, and examined trends in EDS and LDS burning activity for some protected or natural areas where there is information on fire management strategy. This information allows assessment of whether fixed transition dates are appropriate, and where management efforts are appropriate for maintaining a sustainable fire regime.

In the subsequent sections the study area is introduced (section 2.1), the EO data used in the study is described (section 2.2), and the development of the transition date algorithm and decision tree methodology is laid out (sections 2.3 and 2.4). The final part of the methods addresses the definition of areas with intense late season burning (section 2.5) before we present the results in section 3, discuss key findings in section 4 and present conclusions in section 5.

2. Methods

2.1. Area of study

Tropical savannas (including those regularly flooded), defined as savanna occurring within 23.5° north and south of the equator, account for around 11 % of global landmass not permanently frozen (Olson et al., 2001), covering large swathes especially of South America, Africa and Australia. This biome comprises mixed grasslands and woodlands, often characterised by grassy plains and discontinuous woody canopy cover ranging from very sparse to relatively dense (Archibald et al., 2019; Scholes and Archer, 1997). Fires in these regions predominantly occur in the dry season: May - October in the southern hemisphere, November - April in the northern hemisphere (Giglio et al., 2013).

Our assessment focuses on tropical savannas from five core regions: South America north of the equator (NHSA), South America south of the equator (SHSA), Africa south of the equator (SHAF), Africa north of the equator (NHAF), and Australia (AUST). We study fire dynamics for all five core regions and examine burning trends in a handful of protected areas in each. Protected area data were taken from the World Database on Protected Areas (UNEP, 2023). Each of these core regions supports globally significant areas of tropical savannas, in total comprising 92 % of the distribution of tropical savannas and almost 70 % of global fire extent (Table 1). Regional extent and mean annual rainfall for each core region is shown in Fig. 1. Mean annual rainfall is split into bands of 200 mm to highlight regions of low rainfall ($\leq 600 \text{ mm yr}^{-1}$), medium rainfall (600–1000 mm yr^{-1}) and high rainfall ($\geq 1000 \text{ mm yr}^{-1}$). In most cases areas of low rainfall have fire regimes with a longer return interval and more variability, whereas higher rainfall areas experience fires at greater frequency (Archibald et al., 2009) (Figs. 2 and 1).

As we are comparing fire regimes across hemispheres where the wet and dry seasons are out of phase, it is not appropriate to perform analyses exclusively following the calendar year (Boschetti and Roy, 2008). To allow easier comparison across hemispheres, we make reference to a ‘fire year’. In the southern hemisphere the fire year runs from 1st January – 31st December of that year (the fire season remains within the calendar year), and in the northern hemisphere from 1st July of that year – 30th June of the following year (the fire season begins in one calendar year and ends in another). For example, ‘fire year 2010’ refers to the period from 1st January 2010 to 31st December 2010 in the

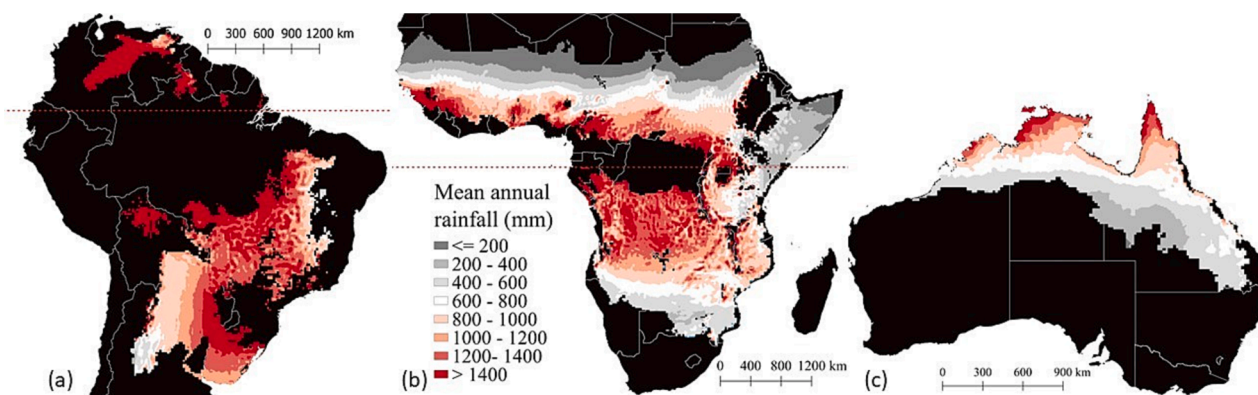


Fig. 1. Global distribution of tropical savannas in (a) South America, (b) Africa and (c) Australia, along with the mean annual rainfall across the period 2003–2021 (Hersbach et al., 2020). The red dotted line in (a) and (b) denotes the equator. (For interpretation of the references to colour in this figure legend, the reader is referred to the web version of this article.)

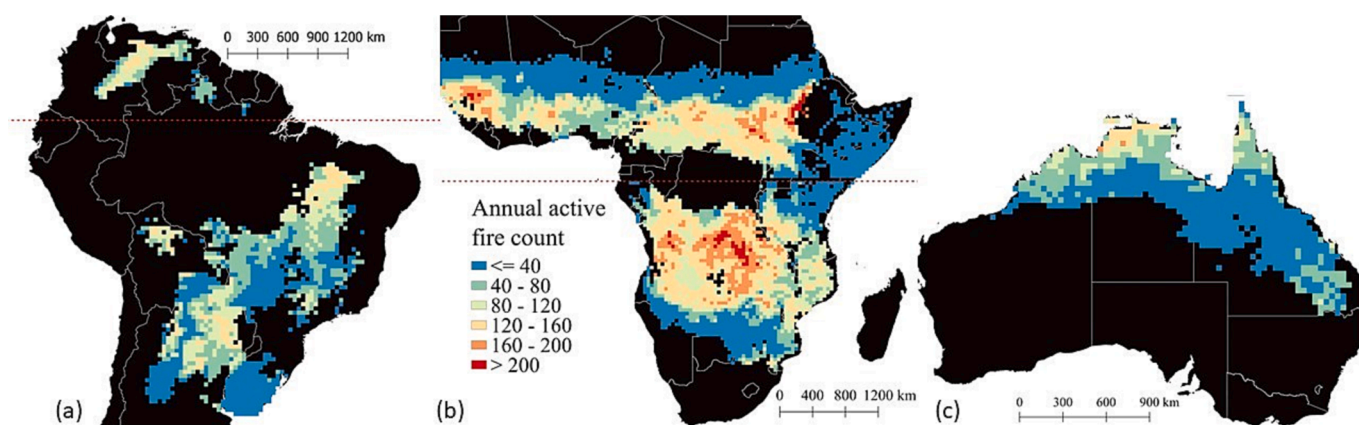


Fig. 2. Total average annual active fire detections from 2003 to 2021 for (a) the South American study region (NNSA & SHSA) (b) the African study region (NNAF & SHAF), and (c) the Australian study region (AUST). The red dotted line represents the equator. Grid cells with less than 40 active fire detections per year (in blue) were excluded from the study. (For interpretation of the references to colour in this figure legend, the reader is referred to the web version of this article.)

southern hemisphere, and 1st July 2010 to 30th June 2011 in the northern hemisphere. This means that our study period for the southern hemisphere was from 1st January 2003 to 31st December 2021, and for the northern hemisphere 1st July 2003 to 30th June 2022 (inclusive).

We do this mostly for ease of comparison across hemispheres and on the assumption that the wet and dry season in the northern hemisphere are exactly 6 months out of phase. This assumption is not totally accurate, not least because this would imply that the fire season in the northern hemisphere should begin on the 2nd July rather than the 1st, but we believe it is appropriate nonetheless as our focus lies in calculating a transition date which by definition must fall somewhere in the middle of the fire season, and will be a relative quantity (i.e. x number of days since the start of the fire year). The fringes of the season with low burning are unlikely to have much effect on determining the EDS to LDS transition date, and a shift in the definition of a fire year by a few days would not change the results meaningfully within a core region. Were the start of a fire year to be changed by a few days, for example, then the transition day-of-year would shift by that number of days, but metrics such as standard deviation would not change.

2.2. Fire data

Active fire data from the Moderate Resolution Imaging Spectroradiometer (MODIS MOD14 collection 6.1, 1 km pixel at nadir (MODIS, 2022)) are available from November 2000 to present. This data is collected daily at regular times: the MODIS instruments are carried on two satellites, Terra and Aqua, each with a day-time overpass (10:30am

for Terra and 1:30 pm for Aqua) as well as a night-time overpass (10:30 pm for Terra and 1:30am for Aqua). Data were downloaded from the start of the first calendar year where both Terra and Aqua data are available (January 2003) up to and including December 2021 (southern hemisphere) and June 2022 (northern hemisphere) in keeping with the fire year definition for each. Hotspot detections from the MODIS instrument rely on the detection of thermal anomalies, either above a given threshold value, or relative to the surroundings, or both (Giglio et al., 2003; Huffman, 2013).

The robustness of our approach is enhanced by a higher number of active fire detections in a given area for a given fire year. To aid this, study regions were split into a relatively coarse grid of $0.5^\circ \times 0.5^\circ$ cells, in which daily count of day-time and night-time hotspots were collected. This allowed more individual detections to be grouped together, while still maintaining a spatial resolution useful enough to intersect with particular geographical features (e.g. national parks or protected areas). Cells with fewer than 40 fire detections per year frequently displayed unrealistic behaviour in the preliminary analysis (e.g. transition dates determined to be in the wet season) and as such all cells below this threshold number of detections were excluded. This number was also selected as a threshold as a sharp geographical boundary is often found around this number, especially in the African core regions. Excluded cells are shown in blue in Fig. 2. Grid cells with significantly more fire detections are highlighted in red.

While active fire data are useful for ascertaining level and timing of fire activity, there are additional burned area products better suited to determining fire extent. The most widely used global burned area

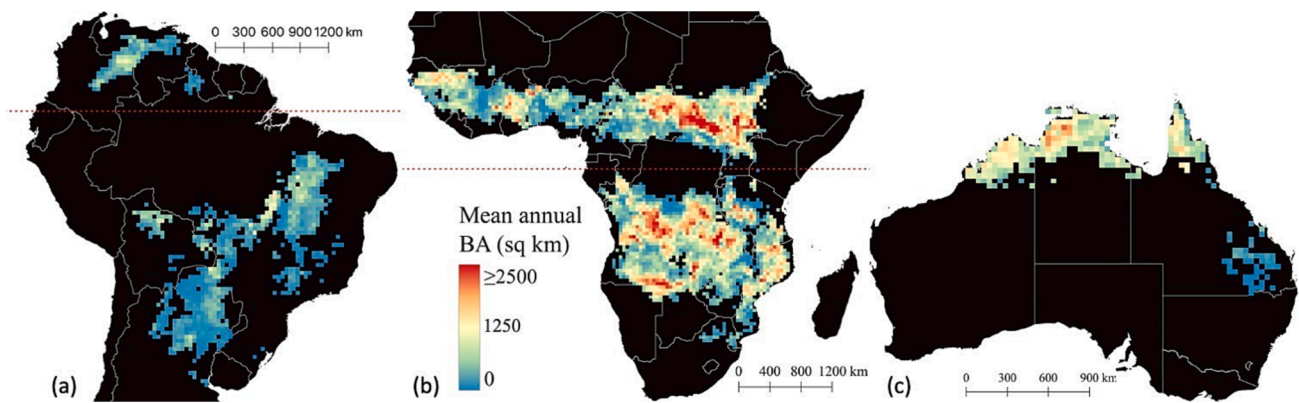


Fig. 3. Total average annual burned area from 2003 to 2021 for (a) the South American study region (NHSA & SHSA) (b) the African study region (NHAF & SHAF), and (c) the Australian study region (AUST). The red dotted line in (a) and (b) denotes the equator. (For interpretation of the references to colour in this figure legend, the reader is referred to the web version of this article.)

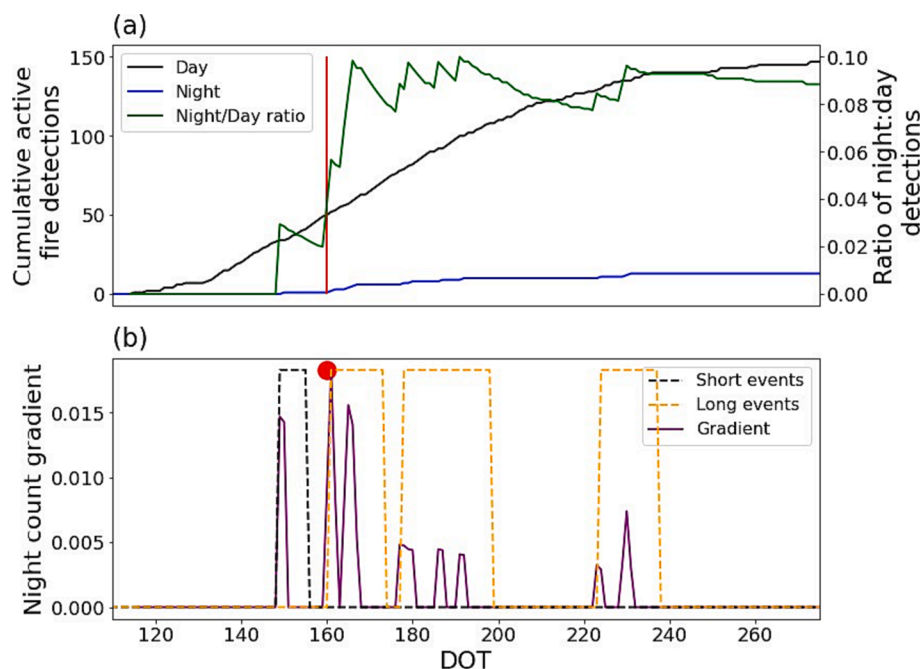


Fig. 4. Example of the method of determining the EDS/LDS transition in one grid cell in central Central African Republic (9°N , 20.5°E , NHAF) for the 2006 fire year. (a) shows the cumulative active fire counts across the year for day and night fires in black and blue respectively, along with the corresponding night:day ratio in green. (b) shows the (positive) gradient of cumulative night fires across the fire year in purple, while the black dotted line indicates activity windows of 7 days or less (ignored) and the orange dotted line longer activity windows. The red dot in (b) shows the location of the maximum gradient in the first valid activity window which becomes the DOT, with a corresponding red vertical line in (a). In this particular case, the DOT is 160, or 8th December. The x-axis is the same for both (a) and (b). (For interpretation of the references to colour in this figure legend, the reader is referred to the web version of this article.)

product is the MCD64A1 product (Giglio et al., 2015) based on data from MODIS instruments. We used Collection 6.1 data, available at a 500 m resolution. The mean annual burned area for the study period is shown in Fig. 3. Burned area data at this scale are provided on a daily basis. For each study region, the date of the EDS to LDS transition as determined from active fire data (see section 2.3) provided a cut-off point before which burned area was classified as occurring in the EDS, and after which in the LDS. This enabled the calculation of the fraction of LDS area burned for each grid cell in the study region.

Additionally, we identify areas where there are varying approaches to fire management, and examine trends in EDS/LDS burned area as a potential result of these practices (Section 3.4). We note that studies have shown this particular product to omit a large portion of small fires in tropical savannas (e.g. Ramo et al., 2021). In making use of this data we therefore are effectively considering burned area from larger fires

(≥ 100 ha) only. This is not the case for the active fire data, as they provide a snapshot of burning activity during the overpass times. In savannas, even fires covering about 0.5 % of an active fire pixel (in the case of MODIS 500 m pixels, around 125 m^2) can be detected (Wooster et al., 2021). Active fire data is already used to augment existing coarse burned area data to include small fires (Werf et al., 2017) thanks to the ability to detect fires significantly smaller than the pixel size (Giglio et al., 2006).

2.3. Transition date algorithm

In this section, we describe the construction of an algorithm which identifies the transition date from EDS to LDS conditions, taking advantage of separate night- and day-time fire detections. While most night fires will occur in the LDS period under more severe burning

Table 2

Per-grid cell averaged statistics for each core region. Standard deviation and LDS fraction means are weighted by the total burned area per grid cell. The excluded grid cells column indicates the fraction of grid cells from each core region that did not meet the 40 fires per year cut off, and in brackets the fraction of the total active fire detections excluded as a result is shown.

core region	Mean annual BA (km ² year ⁻¹)	Mean annual active fire count	Mean standard deviation of DOT (days)	LDS fraction	Excluded grid cells (fire count)
NHSA	317	88	28	64 %	12 % (4 %)
SHSA	251	79	39	71 %	42 % (14 %)
NHAF	827	111	21	62 %	47 % (5 %)
SHAF	885	121	23	61 %	25 % (4 %)
AUST	797	71	54	78 %	62 % (29 %)

conditions, smaller numbers of (less severe) night-time fires also occur in the EDS period (Maier and Russell-Smith, 2012; Govender et al., 2006; Rissi et al., 2017). Here we apply an intuitive approach to defining the EDS to LDS seasonal transition as the rate of increase of night fire relative to day fire activity over the course of a fire season. We define an end to the relatively safe prescribed burning window (end of the EDS) as the date in any fire year when night fires begin to form a significant fraction of all fire detections. To this end, we constructed an algorithm to determine the date of EDS to LDS transition (DOT). Persistence of fires at night is generally attributable to a drying of vegetation and change in conditions consistent with a longer period without rainfall in the LDS; nevertheless, individual night fire detections can occur in the EDS. Often these are isolated events not necessarily related to the seasonal transition, and defining the DOT solely on the basis of the day with the first night-time fire regularly results in erroneous or unrealistic season transitions. To overcome this and define the DOT in a more structured way we apply the concept of an ‘activity window’, which describes separate periods of night-time fire activity using a rolling window of seven days. If one or more night-time fires were detected on a single night and then followed by no detections for the following seven days,

this is defined as a ‘short event’. Any activity window of more than seven days is considered as a ‘long event’. If one or more night-time fires were detected and then followed by a second detection within seven days, then the window is extended until seven full days have elapsed with no active fire detections (see Fig. 4b). In this way, single, random or erroneous fire events were filtered out of the algorithm, and only periods of consistent night-time activity were considered.

This window size is somewhat arbitrary, though through trial and error we found that windows shorter than seven days did not filter out enough erroneous activity in e.g. the wet season and longer windows meant that in some grid cells with fewer active fire detections there was no transition detected at all. The steps of the algorithm were all performed on a cell-by-cell basis unless otherwise stated. A visualisation of this algorithm is shown in Fig. 4 and the approach to define the exact DOT based on these windows is described below.

The first step was to calculate the cumulative annual active fire detections separately for day and night fires (e.g. Fig. 4a). Following this, the gradient of the ratio of day to night fires was calculated to give an indication of the rate of the relative increase of night fires to day fires (i.e. how rapidly night fires become a greater part of total fire activity - shown by the purple line in Fig. 4b). The third step was to split this gradient into long and short activity windows (dotted lines in Fig. 4b), neglecting parts of the gradient falling into short activity windows. The final step was to determine at which date the gradient is at a maximum within the first long activity window. This is the DOT, the point at which night-time fires begin to consistently persist over periods longer than 1 day.

2.4. Decision tree: Drivers of variability

The shift from early to late season fires is a process that happens with the progression of the dry season and is expected to be largely driven by meteorological conditions. For example, lack of rain and lower humidity allows vegetation to dry out, meaning fires can spread more easily and in a sustained way. We examined a variety of these variables (see Table A4)

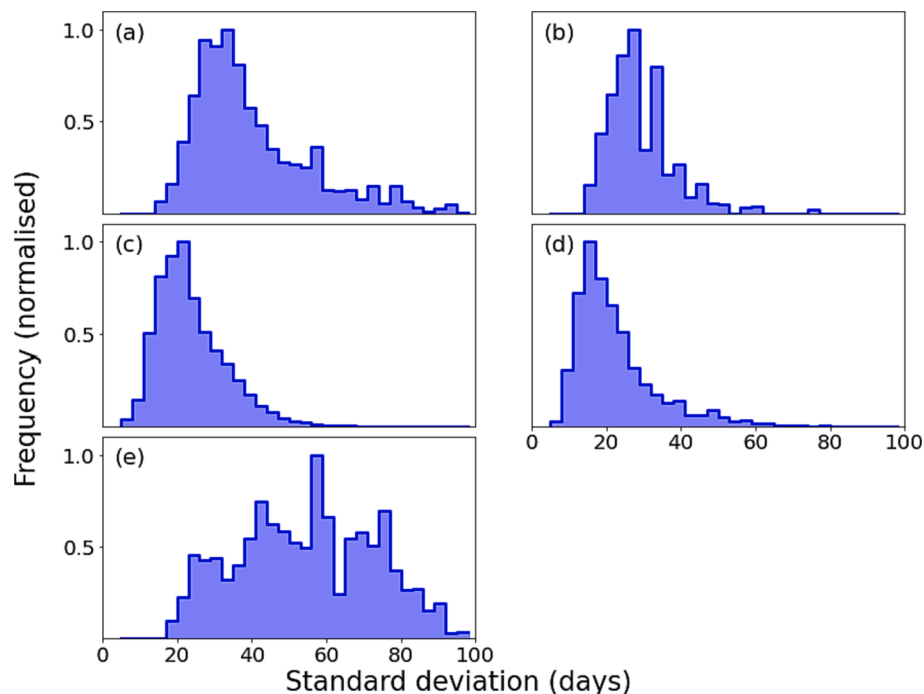


Fig. 5. Mean annual burned area weighted frequency distribution (normalised to the range [0,1]) of the DOT standard deviation for each grid cell in (a) SHSA, (b) NHSA, (c) SHAF, (d) NHAF and (e) AUST. The x-axis ticks indicate the first day of every month. The width of each bar is 3 days. Red dotted lines are placed at 14 days to give an indication of the cut off point for grid cells with relatively consistent DOTs. (For interpretation of the references to colour in this figure legend, the reader is referred to the web version of this article.)

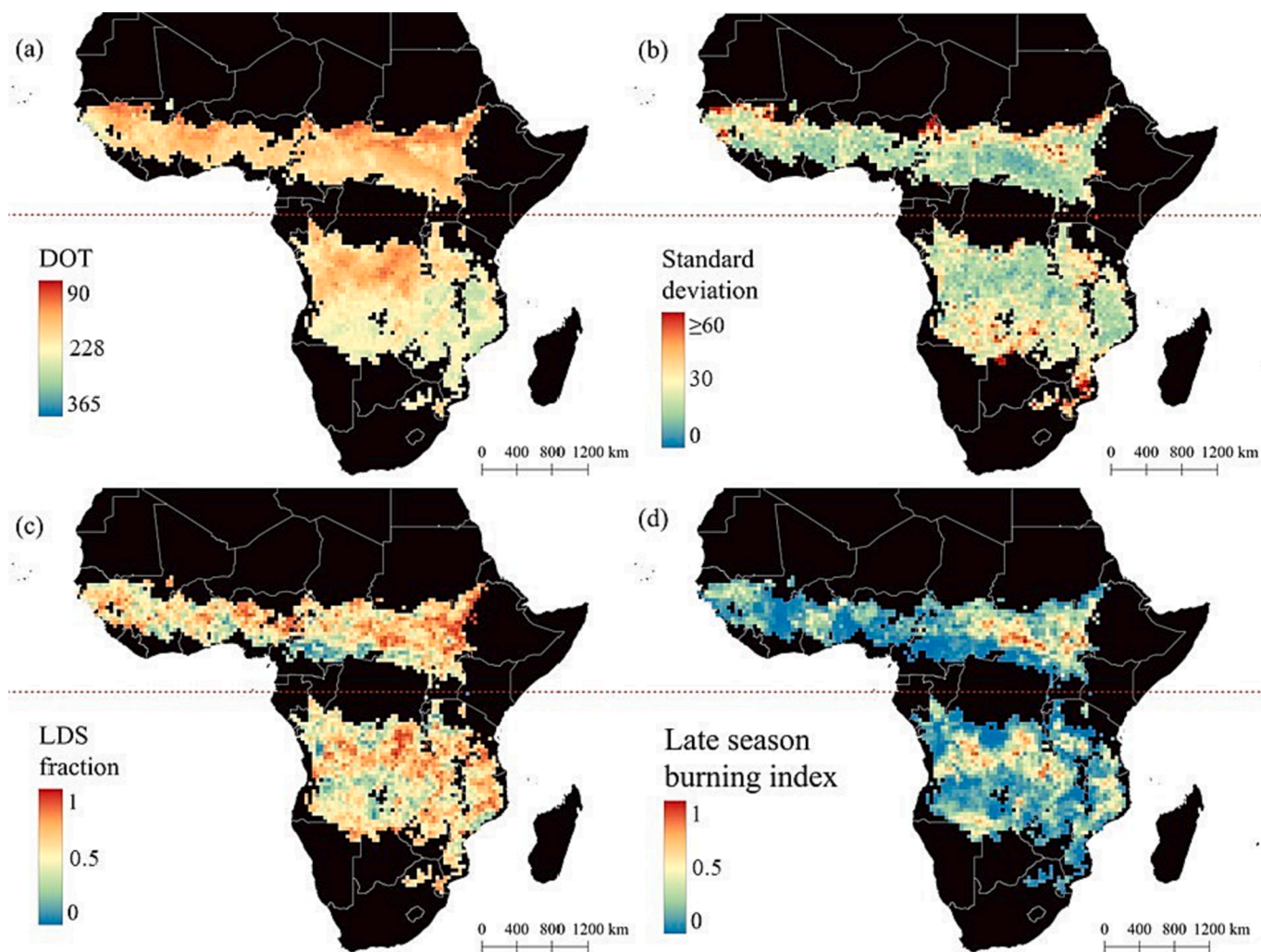


Fig. 6. Maps of both African study regions (NHAF & SHAF) for (a) mean DOT (note that NHAF and SHAF fire years have different start dates), (b) standard deviation in days for (a), (c) the fraction of annual burned area occurring in the LDS, and (d) LSBI. The red dotted line is the equator. (For interpretation of the references to colour in this figure legend, the reader is referred to the web version of this article.)

summed or averaged over 1, 2, 3, 7 and 14 days, and then periods of multiples of 30 days (30, 60, 90 etc) up to 360 days (i.e. periods on the order of days, then weeks, then months), from the DOT backwards in time. As an example, the variable Rainfall 120 in Table 3 refers to the total rainfall summed over the 120 days preceding the DOT. These variables were fed into a random forest regressor in Python (Breiman, 2001; Geurts et al., 2006) in order to identify which variables over which time periods were most significant in explaining the temporal variability of the DOT. In each case, 25 % of the grid cells were kept aside for validation, and statistics presented in the remainder of this paper are based on this validation subset unless stated otherwise.

2.5. Late season burning index and protected areas

With our approach we should be able to identify regions which have significant issues with potentially more damaging late season fires. To that end, we defined a Late Season Burning Index (LSBI) as the normalised product of the LDS fraction and total burned area in a given grid cell (Equation (1)). This is a relative quantity defined to be between 0 and 1, where higher values correspond with a large burned area in a grid cell where most (if not all) of the burning occurs post-DOT, in the LDS.

$$LSBI_i = \frac{\text{Burned area}_i \times \text{LDS fraction}_i - \min(\text{Burned area} \times \text{LDS fraction})}{\max(\text{Burned area} \times \text{LDS fraction}) - \min(\text{Burned area} \times \text{LDS fraction})} \quad (1)$$

Representative protected areas in core regions were examined in the context of this LSBI.

3. Results

3.1. DOT

In this section, we examine patterns spatial and temporal patterns in the DOT. A broad overview is presented in Table 2, showing per-grid cell mean averages across the core regions and study period for a number of variables, which together give an overview of the fire regimes.

3.1.1. Temporal variability

Table 2 shows, amongst other things, the per-grid cell temporally averaged standard deviation of the DOT, weighted by burned area. Standard deviations of three weeks or more in all regions already suggest that DOT is highly variable temporally across the tropical savanna biome. This is expanded on in Fig. 5, which shows the normalised

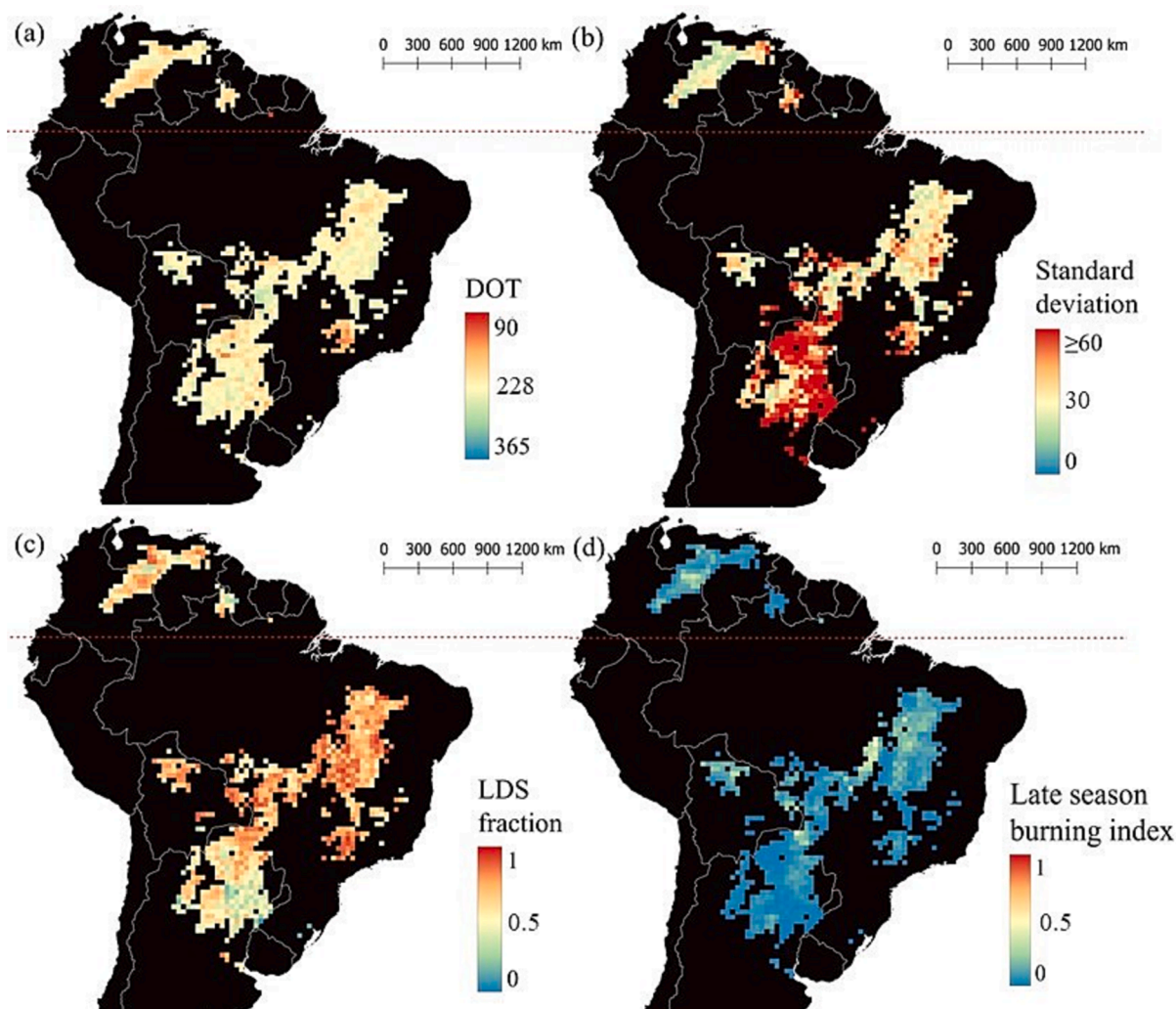


Fig. 7. Maps of both South American study regions (NHSA & SHSA) for (a) mean DOT, standard deviation in days for (a), (c) the fraction of annual burned area occurring in the LDS, and (d) LSBI. The red dotted line is the equator. (For interpretation of the references to colour in this figure legend, the reader is referred to the web version of this article.)

frequency distribution of temporal standard deviations across all grid cells in the five core regions. Most grid cells have a temporally variable DOT, especially in AUST (Fig. 5e) where the fire return times are generally longer (high burned area but low active fire count). Across the study period, cells for which the DOT occurred on roughly similar dates every year were the exception and confined to locations in NHAF and SHAF (Fig. 5c&d).

The lowest temporally variable grid cells in NHAF were found in regions with higher burned area and fire detections (see Fig. 3b), such as in the Central African Republic (CAR), South Sudan and north-western Ghana. Cells with higher variability (standard deviations of 45 days or more) were found sporadically at the Sudan/South Sudan border and along the west coast in Sierra Leone, Guinea/Guinea-Bissau and Mali (dotted along the northernmost edge of Fig. 6b). In SHAF, higher temporal variability was also sporadic and generally found further south, notably in east/central Angola, southern/western Zambia and southern Mozambique (along the southern end of Fig. 6b). The more northerly parts of the region showed lower temporal variability, again corresponding roughly with areas of potentially more intense, LDS burning (Fig. 6c,d).

Generally speaking, temporal DOT variability is higher in South America than in Africa (Fig. 5a,b). The highest variability (60 + days) in SHSA is found further south, though most grid cells in the region show a standard deviation of at least 30 days (Fig. 7b). Above the equator DOT

variability is somewhat lower, though the small relative size of this core region makes it harder to draw comparisons.

There were few grid cells with DOT variability significantly lower than 60 days in AUST, found along the coast of the north-western edge of the Northern Territory and the northernmost tip of Queensland (Fig. 8b), where there is a higher burned area (Fig. 3c). The rest of the core region showed high variability, the highest of any of the core regions, likely linked to the low average number fire detections (Table 2). Much of the AUST region is very low rainfall (Fig. 1) which goes some way to explain why such a significant fraction does not have enough fire detections to be included.

3.1.2. Spatial variability

The distribution of DOTs across the fire year for each core region is shown in Fig. 9. In most cases this distribution reflects the spatial variability in DOT - a prime example of this is found in AUST. DOTs in AUST were spread across most of the dry season from May/June through to September/October, though there is a clear split between earlier DOTs in the western section of the study region (June/July in northern Western Australia and northwest Northern Territory) and later DOTs in the eastern section (August/early September in the northeast Northern Territory and Queensland; Fig. 9e, Fig. 8a).

A similar twin-peak pattern was observed in SHAF (Fig. 9c), where DOTs occurred earlier in the north-west and later further south-east. The

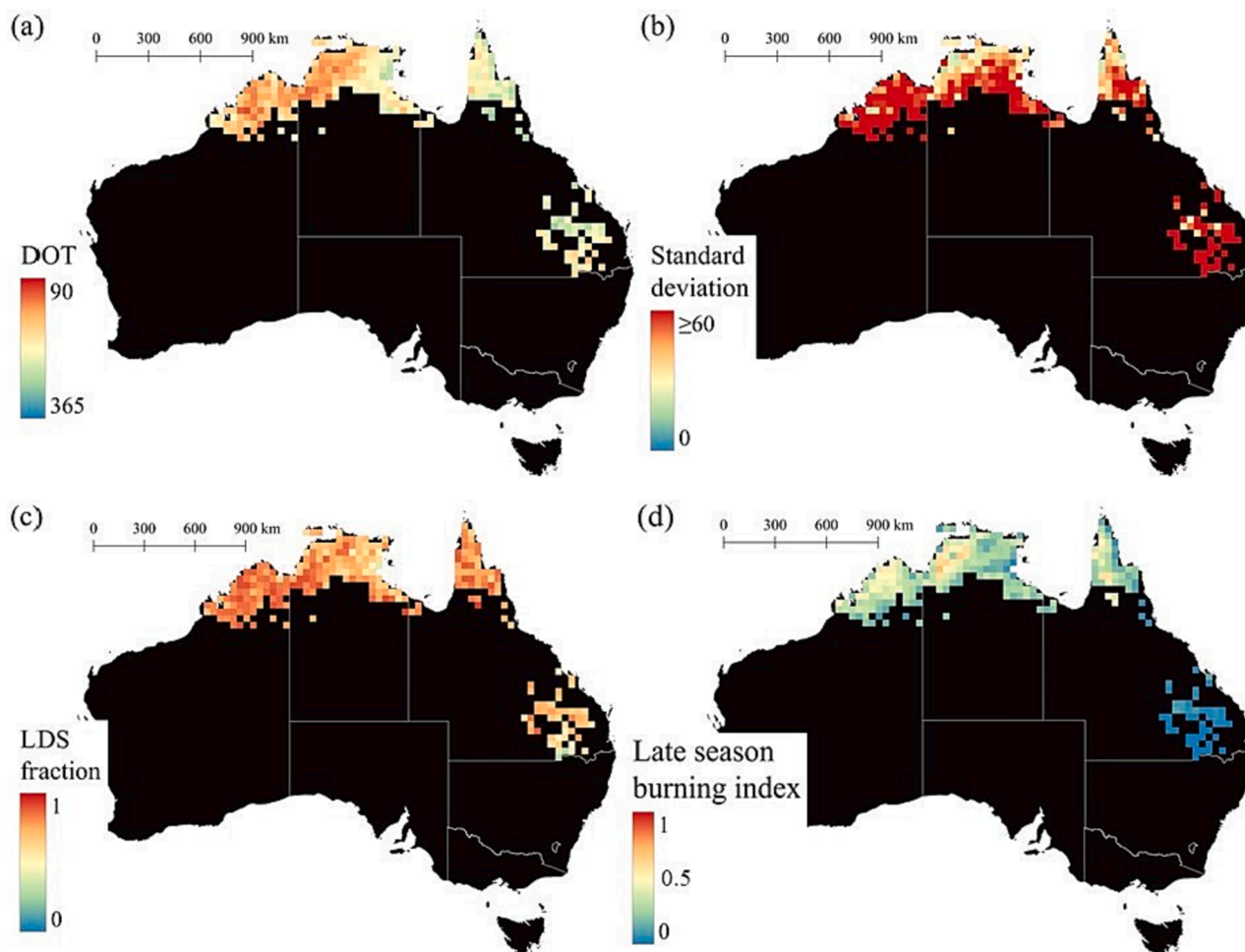


Fig. 8. Maps of the Australian study region (AUST) for (a) mean EDS/LDS transition DOT, (b) standard deviation in days for (a), (c) the fraction of annual burned area occurring in the LDS, and (d) LSBI.

earlier peak around the end of May/start of June are in the area bordering the Congo rainforest. The later peak towards August or September centres more around eastern Zambia and southern Tanzania/northern Mozambique, though notable exceptions include both Kafue national park in west-central Zambia and eastern Niassa reserve in northern Mozambique (6a). NHAf DOT mostly occurs in December or January (Fig. 9d). The northern edge of NHAf tends to show earlier DOTs, particularly in southern Chad and the Sudan/South Sudan border, and later DOTs are found in the far west in Senegal, Sierra Leone and Guinea-Bissau. In South America, earlier DOTs occurred in SHSA only in the southernmost tip of the study region in the state of São Paulo in Brazil and in north-western Paraguay. Most DOTs are in August (Fig. 9a). In NHAf, DOTs are slightly more spread out from late December to early February (Fig. 9b). Later DOTs were found more along the Venezuela/Colombia border, and earlier ones further from that border in both countries (Fig. 7a).

3.2. LDS fraction

Using the DOT as a cut-off date, we classed all MODIS-derived burned area in tropical savannas as either EDS or LDS across the study period.

The total area burned annually for each core region, split into these two categories, is shown in Fig. 10.

In most of the Brazilian section of SHSA LDS fractions were high ($\geq 60\%$) and only in the southern section in Paraguay and northern Argentina did this drop significantly (Fig. 7c). In NHAf the picture is

spatially more mixed, though on average has a lower LDS fraction than SHSA (Table 2). Both SHSA and NHAf show more variance in LDS fraction than the African core regions (Fig. 10a,b). The proportion of area burned in the LDS (LDS fraction) showed minimal temporal variation across the study period in SHAF as a whole (Fig. 10c). There was much spatial variability in this however, with most areas with a high mean annual burned area also showing a higher LDS fraction. A similar pattern was observed in NHAf, temporally consistent (Fig. 10d) while spatially divergent. Especially the frequently burned areas in the east (CAR and South Sudan) show generally higher LDS fractions (Fig. 6c).

The LDS fraction was high across all of AUST, nowhere dropping below 50% except in south-eastern Queensland in the area with the lowest mean annual burned area (Fig. 8c). AUST also had consistently higher LDS fraction than any other study region (Fig. 10e).

Four protected areas were selected as having differing approaches to or challenges in fire management: Bamingui-Bangoran National Park and Biosphere Reserve (northern Central African Republic, NHAf), Mole National Park (northern Ghana, NHAf), Kafue National Park (western Zambia, SHAF) and Kakadu National park (Northern Territory, AUST). In Fig. 11 the LDS fraction of burned area for each of these parks is shown, along with the trend therein. While panels (a) and (b) suggest that the LDS fraction is decreasing for Kakadu and Bamingui-Bangoran, we note that the trend is not (yet) fully significant. A longer series of observations may serve to cement this decreasing trend. The two remaining panels show a relatively steady LDS fraction for Mole and Kafue national parks. All protected areas show relatively large interannual variability.

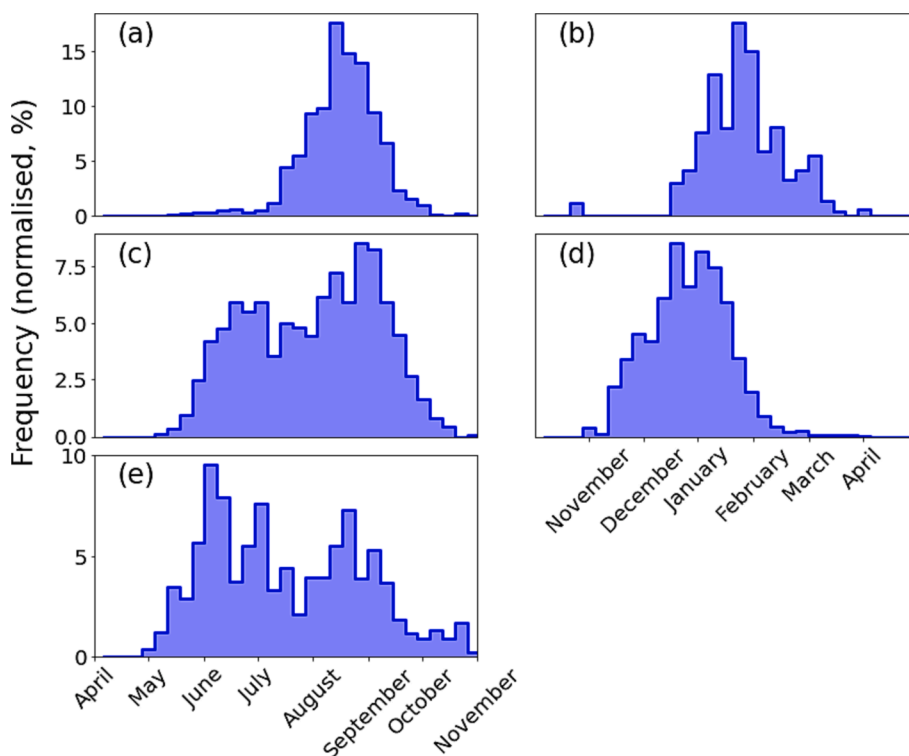


Fig. 9. Mean annual burned area weighted frequency distribution of the mean DOT for each grid cell in (a) SHSA, (b) NHSA, (c) SHAF, (d) NHAF and (e) AUST. The DOT is normalised such that each bar represents a percentage of each core region transitioning from EDS to LDS in that period. The x-axis ticks indicate the first day of every month. The width of each bar is 7 days.

3.3. DOT drivers

Results of the random forest regression model for DOT are shown in Table 3. A full list of variables considered can be found in Table A4 in the Appendix. For SHAF and AUST, just under two-thirds of DOT variability is explained by changes in the total precipitation in the 120 days preceding the DOT. For the other regions it is less dominated by a single variable, though precipitation/evaporation still plays a significant role. NHAF is the only core region where either precipitation or evaporation over the wet season (between 90 and 180 days before DOT) is not one of the two most significant variables.

- these are replaced by vapour pressure deficit. In all cases $r^2 > 0.9$, and RMSE values were between 1 and 2 weeks, indicating a good fit for the models.

3.4. LSBI and protected areas

Most of the South American savanna has a fairly low LSBI due to lower burned area (Fig. 3a), despite a few grid cells with a high LDS fraction. The highest LSBI is just under 0.5, found in and near Araguaia National Park in the Tocantins region of Brazil. AUST has a higher LSBI generally, climbing to 0.6–0.7 in the northwest Northern Territory (around Litchfield National Park, Fish River Conservation area and southwest Kakadu National Park) and the southern end of Cape York (Staaten River National Park and around Harkness Nature Refuge) (Fig. 8d). SHAF continues the trend of higher LSBI values in nature reserves, e.g. in Luando Nature Reserve (central Angola), Kafue National Park (western Zambia) and Niassa Special Reserve (northern Mozambique). High LSBI values (>0.7) are also found outside formally designated protected areas in Haut-Lomami province (southern Democratic Republic of Congo) and Luanda Norte province (northeast Angola). NHAF contains the highest possible LSBI value of 1, in a cluster of high LSBI grid cells (0.8–1) between Chinko Nature Reserve/Zemongo Faunal Reserve in Central African Republic and Southern National Park

in South Sudan (Fig. 6d & Fig. 12).

4. Discussion

4.1. Seasonality

There is a clear connection between higher fire activity and lower temporal DOT variability across all 5 core regions. This also holds true, albeit slightly less clearly, for the connection between high fire activity and higher LDS fraction. In general we find lower temporal variability in DOT and a higher proportion of area burned in the LDS in frequently burned grid cells (most strongly observed in SHAF and NHAF). That temporal DOT variability and fire frequency are strongly connected is not surprising given that the method of determining the DOT becomes more reliable as the number of fire detections in a grid cell increases. The fact that areas with a higher LDS fraction also show a higher burned area lends credibility to the approach as LDS fires tend to be more spatially extensive.

It is not often the case, however, that a grid cell exhibits low enough variability to be considered as having a more or less ‘fixed’ DOT. Very few grid cells were found to have a standard deviation of 10 days or less, and these are only found in Africa; specifically, in the north-western section of SHAF (southern DRC, eastern/central Angola and northern Zambia) and in the east-central region of NHAF (CAR, South Sudan) and one or two other cells dotted around the western side of the region. This cluster in NHAF is the only true grouping of lower variability grid cells, with the rest described by single or cell pairs. Even places with very frequent fires exhibit standard deviations generally ≥ 15 –20 days. The conclusion is that fixed transition dates may be practical to use in in-situ fire management protocols, but they do not reflect the temporal fire dynamics of most, if not all, savanna regions. The temporal spread in the distribution of burned area-weighted DOT in Fig. 9 is likely related to the geographical distribution of frequently burning areas. If burning is concentrated largely within a relatively small area in the core region (e.

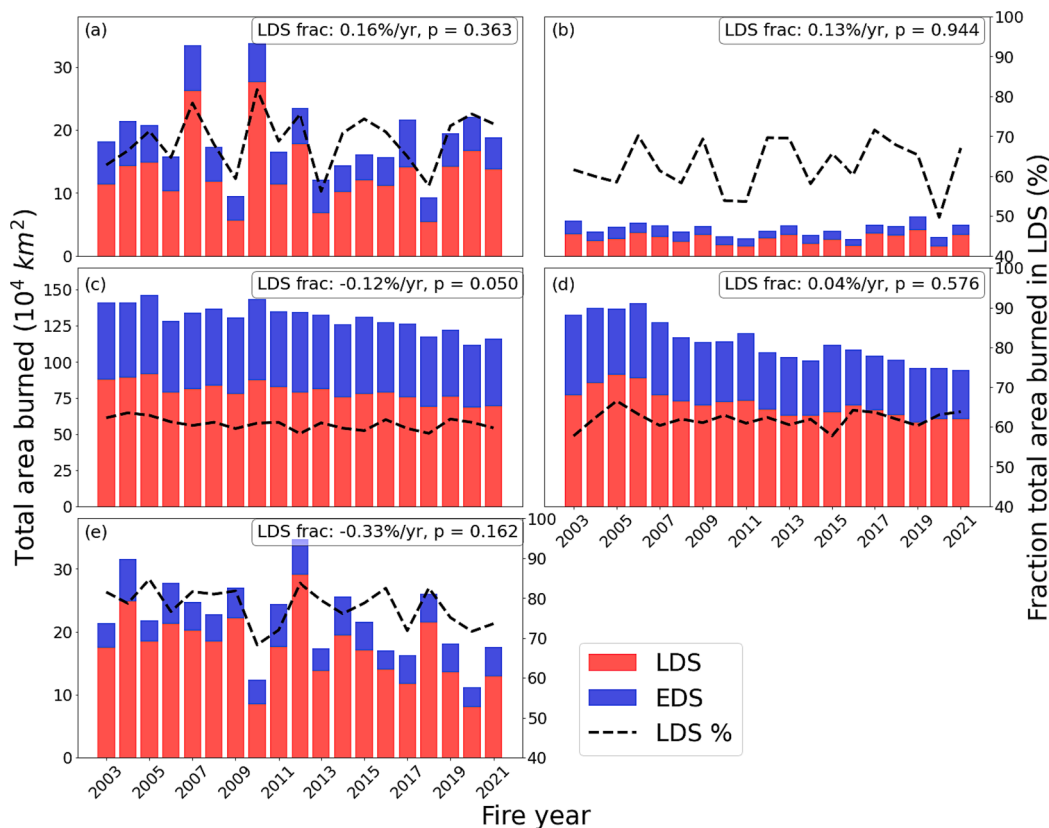


Fig. 10. Total burned area in the EDS (blue) and LDS (red) in (a) SHSA, (b) NHSA, SHAF, (d) NHAf and (e) AUST in grid cells with ≥ 40 active fire detections per year. Black dotted line shows the % of burned area occurring in the LDS, with the trend over the study period displayed in upper right-hand corner of each plot. None of the trends are significant, as shown by the p-value. (For interpretation of the references to colour in this figure legend, the reader is referred to the web version of this article.)

g. NHSA, SHSA and NHAf, Fig. 9a, b, d), then the histogram peak is more distinct. SHAF and AUST have several areas of more concentrated burning spread across the core region (Fig. 3b, c), reflected by a more distributed weighted DOT - though these areas are also larger in size than in particular NHSA, allowing for more variation. NHAF is the largest study region, though burned area is largely concentrated around the Central African Republic and both Sudans, resulting in a relatively narrower DOT distribution for the core region despite its size. Again, even in core regions with a smaller transition window (Fig. 9) still have a spread of two or more months, meaning that the use of a fixed transition date for one of these core regions does not reflect the reality on the ground.

While relatively few fires are undetected by active fire products (even those with coarse resolution) (Wooster et al., 2021; Giglio et al., 2006) this analysis omits a potentially large amount of burned area in the form of small fires (< 100 ha). The small fire fraction of burned area is generally expected to be higher outside of peak burning season (i.e. generally higher in the EDS than in the LDS - (Ramo et al., 2021; Perry et al., 2019). This effect appears to be more pronounced in areas with higher rainfall (Perry et al., 2019) as more moist conditions in the EDS in those regions limit the spread of fire. However, (Ramo et al., 2021) also suggests that at least in the case of Africa the BA missed as a result of coarser resolution in the MODIS product is relatively well-distributed across the fire season. This would imply that while the total amount of BA is higher in reality than what is shown in Fig. 10; the LDS fraction may not change dramatically as a result of using higher resolution data. It is also unlikely to change the actual transition dates significantly, as smaller fires will likely have a shorter duration, making them more likely to ignite and then extinguish in the time between MODIS overpasses, and thus avoid detection. There is much opportunity for

undetected burning between the 1:30 pm and 10:30 pm overpass times. As soon as fires do persist overnight they are more likely to be detected by either the 10:30 pm or 1:30am overpass times. We therefore expect the moment of increase in night-time detections that our algorithm uses to define the DOT to remain relatively consistent.

4.2. Meteorological drivers

Many different potential drivers of variability in DOT in global savannas were examined in the context of the DOT. Due to the size of the grid cell however, ascribing connections between the general meteorological conditions in the entire cell and a fire event that occurs under potentially divergent local meteorological conditions is potentially problematic. As an example, it may be that fire activity is concentrated within a small segment of a grid cell, where meteorological conditions are locally divergent from “representative” grid cell weather data. Meteorological variables over fixed periods (e.g. total precipitation in January through March) proved also to be largely ineffective at explaining variability in DOT, though flexible periods (e.g. total metres of water equivalent evaporated in the 60 days preceding the DOT) had much higher correlations with DOT. This means that making predictions year-on-year on the basis of these variables is a challenge; however, we can at least get a sense of what the most important factors are in driving inter-annual DOT variability from region to region. The most important period of time in terms of driving DOT variability across all study regions was about 90–180 days (3–6 months) before DOT, in almost all cases constituting the bulk of the preceding wet season. Although shorter period variables were not irrelevant (see especially solar radiation in the 24 h preceding DOT in SHSA), currently the development of less severe and cooler fires in the EDS into hotter, longer-lived and more

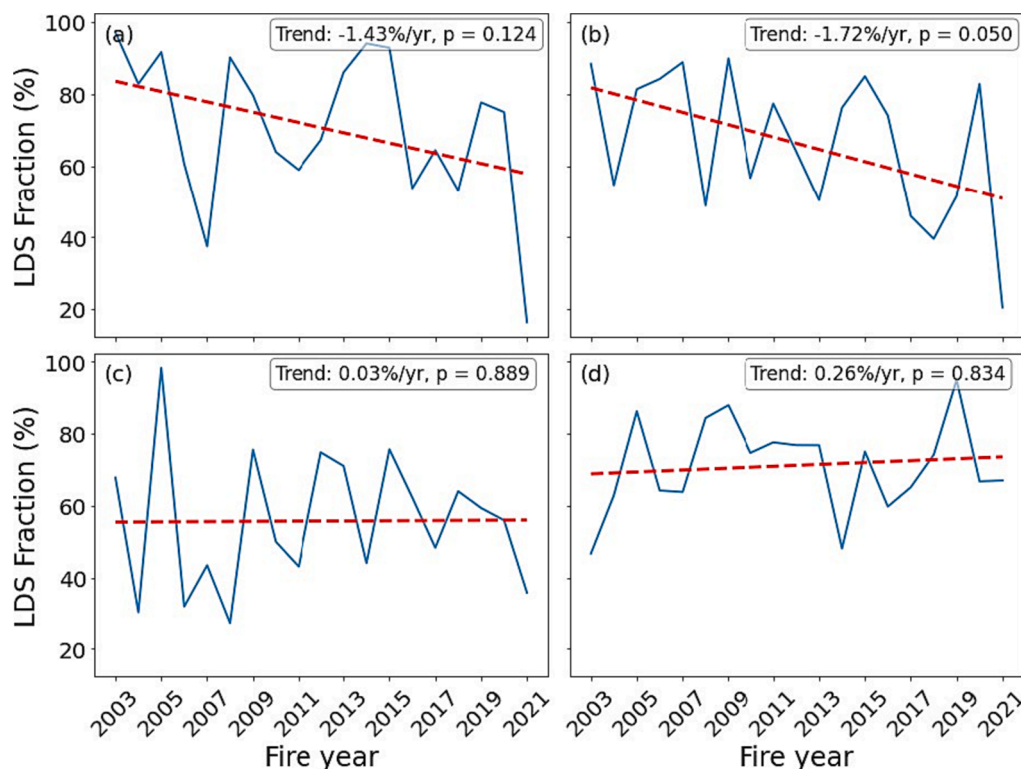


Fig. 11. LDS fraction and trend in 4 parks with annual burning and different approaches to fire management: (a) Kakadu National park, (b) Bamingui-Bangoran National Park and Biosphere Reserve (c) Mole National Park and (d) Kafue National Park. Trends of LDS fraction are shown in the top right corner of each panel. The significance of each trend is shown in the p-value.

Table 3

Two most important variables according to Random Forest models for each core region. The number after each variable refers to the number of days before DOT that the variable is summed (Rainfall, Evaporation, Surface Solar Downward Radiation) or averaged (Vapour Pressure Deficit) over. Shown for each variable is the feature importance (a percentage of the DOT variance explained by that variable) and the correlation with the DOT (r). Also shown is the performance of the model on validation data for each region, in the form of an r^2 and root mean squared error (RMSE).

core region	Variable 1 (importance, r)	Variable 2 (importance, r)	r^2	RMSE (days)
NHSA	Rainfall 180 (14 %, -0.71)	Evaporation 90 (9 %, 0.60)	0.90	12.92
SHSA	Evaporation 180 (37 %, 0.68)	Surface Solar Radiation Downwards 1 (11 %, 0.51)	0.97	9.33
NHAF	Vapour Pressure Deficit 90 (26 %, 0.77)	Dew Point 120 (16 %, 0.76)	0.96	6.80
SHAF	Rainfall 120 (61 %, -0.81)	Surface Solar Radiation Downwards 30 (10 %, 0.50)	0.96	9.36
AUST	Rainfall 150 (63 %, -0.73)	Surface Solar Radiation Downwards 210 (8 %, -0.54)	0.98	11.01

severe in the LDS appears to be determined more so by activity during the wet season than by, for example, a rapid drying out of the fuel due to heatwaves or similar events. Fuel load (and by inference fuel connectivity) is moisture-limited in most of the savanna biome up to about 1200 mm/year of rainfall (Lehmann et al., 2011; Archibald et al., 2009), so poor rains during the wet season may limit fuel growth, restricting fuel connectivity and thus fire spread.

This conclusion is supported by the fact that most of the prominent

identified variables are directly moisture-related (rainfall or humidity), and rainfall variables were always strongly negatively correlated with DOT (i.e. more rain means an earlier DOT). Further support is lent by the fact that DOTs in core regions with a higher degree of aridity (e.g. AUST) are more strongly linked to rainfall in the growing season. Fuel growth in less arid core regions is not as rainfall-limited as it is in more arid regions - more rain in the wet season results in greater fuel growth and increased fire spread earlier in the dry season. This is also observed internally in SHAF, where higher rainfall areas in the northwest section of the study region tend to have an earlier DOT than other, lower rainfall areas (Fig. 6a). It appears that fuel connectivity/fuel load is a better predictor of DOT than fuel condition.

4.3. Late season burning index

More often than not, areas with high LSBI correspond (roughly) to reserves, national parks, or other protected nature areas - especially in the African study region, where the highest LSBI values are found. This is illustrated with a few examples in Fig. 12. As discussed in the previous section (4.2), it appears that fuel connectivity is key in allowing fires to spread in general, and earlier in the season. Protected areas are areas where development and the human footprint is deliberately limited, so fewer barriers prevent fires from spreading further (Archibald et al., 2010; Archibald et al., 2009). These are areas where active management is a necessity to lower the impact of spatially extensive LDS fires.

LSBI calculation is constructed essentially from two terms (Equation (1)), each with some degree of uncertainty. The uncertainty in the BA term, particularly pertaining to small fires, has been given some consideration earlier in this discussion (Section 4.1). Pertaining to LSBI, areas with higher BA/larger fires (such as protected areas) from MODIS have similar BA to higher resolution data (Ramo et al., 2021), so LSBI for these areas is unlikely to change as a result of this uncertainty. Other areas where a higher proportion of BA comes from small fires would see

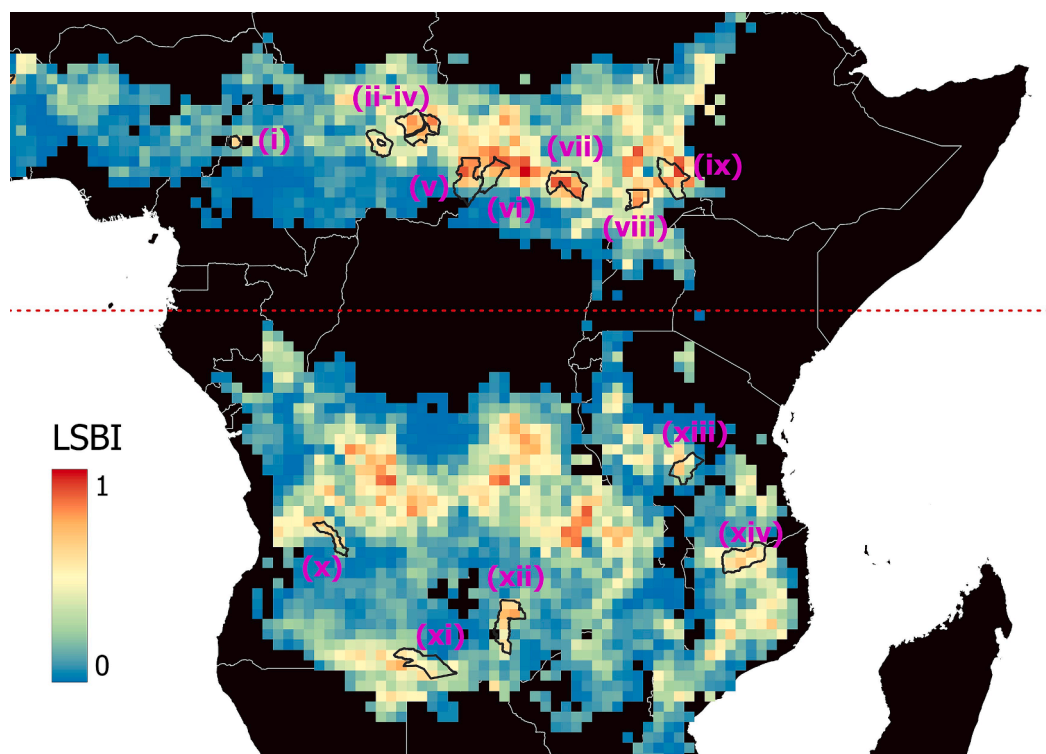


Fig. 12. LSBI in the African study region with various protected areas highlighted: (i) Faro National Park (Cameroon), (ii-iv) Bamingui-Bangoran National Park and Biosphere Reserve, Manovo-Gounda-Saint Floris National Park & Ouandija-Vakaga Faunal Reserve (left-right, Central African Republic), (v) Chinko National Park (Central African Republic), (vi) Zemongo Faunal Reserve (Central African Republic), (vii) Southern National Park (South Sudan), (viii) Badilingo National Park (South Sudan) (ix) Boma National Park (South Sudan), (x) Integral Nature Reserve and the Luando (Angola), (xi) Luengue- Liuana National Park (Angola), (xii) Kafue National Park (Zambia), (xiii) Ruaha National Park (Tanzania) and (xiv) Niassa Special Reserve (Mozambique). Information on protected areas was taken from the World Database on Protected Areas (UNEP, 2023).

their LSBI increase somewhat. This effect will not scale linearly, however, as LSBI is a relative quantity, and as such the effect of the BA uncertainty on LSBI will be dampened. The effect of higher resolution BA on the LDS fraction is also touched upon in Section 4.1. While there is some uncertainty from this source, we expect this too to be of limited effect due also in part to the relative nature of the definition of LSBI.

4.4. Local management and EDS burning

National parks and protected areas are often more active in terms of wildfires than other areas (as discussed in section 4.3; see also Fig. 12), and provide opportunities for local insight into the seasonal skew of burning. For example, managers in Kakadu National Park (AUST, Fig. 11a) have been engaged in a revival of traditional fire practices associated with Aboriginal Australian culture (EDS burning) for many years (see for example <https://www.isfmi.org/new-page-1> or <https://parksaustralia.gov.au/kakadu/discover/culture/country/>), and this appears to have paid dividends in terms of the falling fraction of fires occurring in the LDS. Mole National Park in northern Ghana (NHAF) faces increasing issues including but not limited to poaching and encroachment from population surrounding the park (e.g. (Domfeh et al., 2023), and references therein). However, much of the community within the park partakes in EDS burning for agricultural purposes (Sackey and Hale, 2008), so this may help prevent burning within Mole becoming too skewed towards the LDS (Fig. 11c). Kafue National Park (western Zambia, SHAF) promotes EDS burning, though also faces encroachment from local populations (Authors observations & personal communication from park management), which may explain why there has been a small increase in the LDS fraction over the study period (Fig. 11d). Bamingui-Bangoran National Park (northern Central African republic, NHAF) is an interesting case as the region is sparsely populated

and has relatively little management input from government or other official bodies (Foundation, 2020) (and references therein), and yet exhibits a declining trend in LDS fraction (Fig. 11b). There is evidence of incursions from pastoral communities from bordering countries, as well as suggestions that rebel groups have used the area as a refuge (Bank, 2010). Activity from these groups may have influenced the fire regime in the EDS somehow, but this remains speculation.

5. Conclusions

In this paper we have described a new approach for defining the transition between the early and late dry seasons in tropical savannas globally, based on assessment of the ratio between day-time to night-time active fire hotspots (Figs. 6-8a). Based on the definition of DOT we split fire activity into a clearly-defined early and late dry seasons (Fig. 10), identified areas with greater fire activity skewed towards the LDS (LSBI, Figs. 6- 8d, 12), and examined a few examples of management approaches/challenges within regional protected areas (section 4.4). Almost all areas showed DOT variability of more than 14 days (Figs. 6-8b), indicating that while fixed transition dates provide practical benchmarks, they do not represent inter-annual reality. While predictions of future DOTs proved challenging, the development of a NRT model to assess when the DOT has occurred is feasible and could provide valuable information for management instances in global tropical savannas.

Investigation of protected areas within the tropical savanna biome suggested that those areas with more significant management input and/or facing fewer challenges have more success in reducing burned area in the LDS. We expect that continuity of these management approaches will allow more detailed investigation of the efficacy of given management techniques in the tropical savannas.

Table A4

Full feature description for Random Forest regressor. All means and sums were taken of daily variables unless explicitly stated otherwise. Data is available from the ERA5-Land database (J. Muñoz Sabater, ERA5-Land hourly data from, 1981).

Feature Name	Description	Feature source	Units
Rainfall	Total rainfall summed over 1, 2, 3, 7, 14, 30, 60, 90, 120, 150, 180, 210, 240, 270, 300, 330 and 360 days previous to the DOT	ERA-5 Land	<i>m water equivalent</i>
Evaporation	Total evaporation summed over 1, 2, 3, 7, 14, 30, 60, 90, 120, 150, 180, 210, 240, 270, 300, 330 and 360 days previous to the DOT	ERA-5 Land	<i>m water equivalent</i>
SSRD	Total downward surface solar radiation summed over 1, 2, 3, 7, 14, 30, 60, 90, 120, 150, 180, 210, 240, 270, 300, 330 and 360 days previous to the DOT	ERA-5 Land	Jm^{-2}
STR	Total surface thermal radiation summed over 1, 2, 3, 7, 14, 30, 60, 90, 120, 150, 180, 210, 240, 270, 300, 330 and 360 days previous to the DOT	ERA-5 Land	Jm^{-2}
SWVL1	Mean soil water volume 0-7cm below surface averaged over 1, 2, 3, 7, 14, 30, 60, 90, 120, 150, 180, 210, 240, 270, 300, 330 and 360 days previous to the DOT	ERA-5 Land	m^3m^{-3}
T2M	Mean 2m temperature averaged over 1, 2, 3, 7, 14, 30, 60, 90, 120, 150, 180, 210, 240, 270, 300, 330 and 360 days previous to the DOT	ERA-5 Land	<i>K</i>
D2M	Mean 2m dewpoint temperature averaged over 1, 2, 3, 7, 14, 30, 60, 90, 120, 150, 180, 210, 240, 270, 300, 330 and 360 days previous to the DOT	ERA-5 Land	<i>K</i>
VPD	Mean surface vapour pressure deficit averaged over 1, 2, 3, 7, 14, 30, 60, 90, 120, 150, 180, 210, 240, 270, 300, 330 and 360 days previous to the DOT	ERA-5 Land	<i>kPa</i>
RH	Mean relative humidity averaged over 1, 2, 3, 7, 14, 30, 60, 90, 120, 150, 180, 210, 240, 270, 300, 330 and 360 days previous to the DOT	ERA-5 Land	%

While further research is needed on the drivers of DOT variability, we were able to demonstrate that there is a link between more rain, higher fuel load/connectivity, and an earlier DOT, as well as with a higher LDS fire fraction. Annual DOT appears to best reflect the development of continuous fuel loads under favourable wet season conditions.

CRedit authorship contribution statement

Tom Eames: Conceptualization, Software, Investigation, Formal analysis, Writing – original draft. **Roland Vernooij:** Conceptualization, Investigation. **Jeremy Russell-Smith:** Conceptualization, Writing – review & editing, Supervision. **Cameron Yates:** Conceptualization, Writing – review & editing. **Andrew Edwards:** Conceptualization, Writing – review & editing. **Guido R. van der Werf:** Conceptualization, Writing – review & editing, Funding acquisition, Supervision.

Declaration of competing interest

The authors declare that they have no known competing financial interests or personal relationships that could have appeared to influence the work reported in this paper.

Data availability

Data will be made available on request.

Acknowledgements

This research was carried out with support of the 2017 Ammodo Science Award for Natural Sciences.

Appendix A. . Decision tree variables

See Table A4.

References

- Andela, N., Morton, D.C., Giglio, L., Paugam, R., Chen, Y., Hantson, S., Werf, G.R.V.D., Anderson, J.T., 2019. The Global Fire Atlas of individual fire size, duration, speed and direction. *Earth Syst. Sci. Data* 11, 529–552. <https://doi.org/10.5194/essd-11-529-2019>.
- Archibald, S., Roy, D.P., van Wilgen, B.W., Scholes, R.J., 2009. What limits fire? An Examination of Drivers of Burnt Area in Southern Africa. *Global Change Biology* 15, 613–630. <https://doi.org/10.1111/j.1365-2486.2008.01754.x>.
- Archibald, S., Scholes, R.J., Roy, D.P., Roberts, G., Boschetti, L., 2010. Southern African fire regimes as revealed by remote sensing. *Int. J. Wildland Fire* 19, 861–878. <https://doi.org/10.1071/WF10008>.
- Archibald, S., Bond, W.J., Hoffmann, W., Lehmann, C., Staver, C., Stevens, N., 2019. *Distribution and Determinants of Savannas. Savanna Woody Plants and Large Herbivores*, Wiley, in, pp. 1–24.
- W. Bank Central African Republic Country Environmental Analysis : Environmental Management for Sustainable Growth 2010.
- A.C.S. Barradas M. Borges M.M. Costa Plano de manejo integrado do fogo – Esta,ção Ecológica Serra Geral do 2018 Tocantins, ICMBIO.
- Beerling, D.J., Osborne, C.P., 2006. The origin of the savanna biome. *Glob. Chang. Biol.* 12, 2023–2031. <https://doi.org/10.1111/j.1365-2486.2006.01239.x>.
- L. Boschetti, D. P. Roy, Defining a fire year for reporting and analysis of global interannual fire variability, *Journal of Geophysical Research: Biogeosciences* 113 (9) 2008. doi:10.1029/2008JG000686.
- Breiman, L., 2001. *Random Forests*. *Mach. Learn.* 45, 5–32.
- Butz, R.J., 2009. Traditional fire management: historical fire regimes and land use change in pastoral East Africa. *Int. J. Wildland Fire* 18, 442. <https://doi.org/10.1071/wf07067>.
- Chief, B.H.W., Frost, P.G.H., Robertson, F., 1987. The Ecological Effects of Fire in Savannas 93–140. <https://www.researchgate.net/publication/247848261>.
- Domfeh, M.K., Sey, N.E.N., Amproche, A.A., Mortey, E.M., Antwi-Agyei, P., Nyantakyi, E.K., 2023. Exploring key drivers of forest fires in the Mole National Park of Ghana using geospatial tools. *Spatial Information Research* 31, 27–37. <https://doi.org/10.1007/s41324-022-00478-x>.
- Edwards, A.C., Maier, S.W., Hutley, L.B., Williams, R.J., Russell-Smith, J., 2013. Spectral analysis of fire severity in north Australian tropical savannas. *Remote Sensing of Environment* 136 56–65. <https://doi.org/10.1016/j.rse.2013.04.013>.
- Eriksen, C., 2007. Why do they burn the 'bush'? Fire, Rural Livelihoods, and Conservation in Zambia, *Geographical Journal* 173, 242–256. <https://doi.org/10.1111/j.1475-4959.2007.00239.x>.
- Fitzsimons, J., Russell-Smith, J., James, G., Vigilante, T., Lipsett-Moore, G., Morrison, J., Looker, M., 2012. Insights into the biodiversity and social benchmarking components of the Northern Australian fire management and carbon abatement programmes. *Ecol. Manag. Restor.* 13, 51–57. <https://doi.org/10.1111/j.1442-8903.2011.00624.x>.
- G.C. Foundation Country Profile: Central African Republic 2020.
- Gambiza, J., Campbell, B.M., Moe, S.R., Frost, P.G.H., 2005. Fire behaviour in a semi-arid *Baikiaea Plurijuga* savanna woodland on Kalahari sands in western Zimbabwe. *S. Afr. J. Sci.* 101, 239–244.
- M. Garde B.L. Nadjamerrek M. Kolkkiwarra J. Kalarriya J. Djand-jomerr, B. Birriyabirriya, R. Bilindja, M. Kubarkku, P. Biless, The language of fire: seasonality, resources and landscape burning on the Arnhem Land plateau Culture, Ecology and Economy of Fire Management in North Australian Savannas : Rekindling the Wurrk Tradition 2009 CSIRO Publishing 85 164.
- Geurts, P., Ernst, D., Wehenkel, L., 2006. Extremely randomized trees. *Mach. Learn.* 63, 3–42. <https://doi.org/10.1007/s10994-006-6226-1>.
- Gibson, R., Danaher, T., Hehir, W., Collins, L., 2020. A remote sensing approach to mapping fire severity in south-eastern Australia using sentinel 2 and random forest. *Remote Sens. Environ.* 240, 111702 <https://doi.org/10.1016/j.rse.2020.111702>.
- Giglio, L., Desloires, J., Justice, C.O., Kaufman, Y.J., 2003. An enhanced contextual fire detection algorithm for MODIS. *Remote Sensing of Environment* 87, 273–282. [https://doi.org/10.1016/S0034-4257\(03\)00184-6](https://doi.org/10.1016/S0034-4257(03)00184-6).
- L. Giglio G.R. van der Werf J.T. Randerson G.J. Collatz P. Ka-sibhatla, Global estimation of burned area using modis active fire observations *Atmospheric Chemistry and Physics* 6 2006 957 974 10.5194/acp-6-957-2006.
- L. Giglio, C. Justice, L. Boschetti, D. Roy, MCD64A1 MODIS/Terra+Aqua Burned Area Monthly L3 Global 500m SIN Grid V006, distributed by NASA EOSDIS Land Processes DAAC (2015). doi:<https://doi.org/10.5067/MODIS/MCD64A1.006>.
- Giglio, L., Randerson, J.T., Werf, G.R.V.D., 2013. Analysis of daily, monthly, and annual burned area using the fourth-generation global fire emissions database (GFED4), *Journal of Geophysical Research: Biogeosciences* 118, 317–328. <https://doi.org/10.1002/jgrg.20042>.
- Giglio, L., Schroeder, W., Justice, C.O., 2016. The collection 6 MODIS active fire detection algorithm and fire products. *Remote Sensing of Environment* 178, 31–41. <https://doi.org/10.1016/j.rse.2016.02.054>.
- Giglio, L., Boschetti, L., Roy, D.P., Humber, M.L., Justice, C.O., 2018. The collection 6 modis burned area mapping algorithm and product. *Remote Sens. Environ.* 217, 72–85. <https://doi.org/10.1016/j.rse.2018.08.005>.
- Govender, N., Trollope, W.S., Wilgen, B.W.V., 2006. The effect of fire season, fire frequency, rainfall and management on fire intensity in savanna vegetation in South Africa. *J. Appl. Ecol.* 43, 748–758. <https://doi.org/10.1111/j.1365-2664.2006.01184.x>.
- Groom, P.K., Lamont, B., 2015. *Plant Life of Southwestern Australia : Adaptations for Survival*. Walter de Gruyter.
- H. Hershbach B. Bell P. Berrisford S. Hirahara A. Hořanyi, J. Muñoz-Sabater, J. Nicolas, C. Peubey, R. Radu, D. Schepers, A. Simmons, C. Soci, S. Abdalla, X. Abellan, G. Balsamo, P. Bechtold, G. Biavati, J. Bidlot, M. Bonavita, G. D. Chiara, P. Dahlgren, D. Dee, M. Dia-mantakis, R. Dragani, J. Flemming, R. Forbes, M. Fuentes, A. Geer, L. Haimberger, S. Healy, R. J. Hogan, E. Hölm, M. Janisková, S. Keeley, P. Laloyaux, P. Lopez, C. Lupu, G. Radnoti, P. de Rosnay, I. Rozum, F. Vamborg, S. Villaume, J. N. Thepaut, The ERA5 global reanalysis Quarterly *Journal of the Royal Meteorological Society* 146 2020 1999 2049 10.1002/qj.3803.
- R. Hill A. Baird D. Buchanan Aborigines and fire in the wet tropics of Queensland, Australia: Ecosystem management across cultures *Society and Natural Resources* 12 1999 205 223 10.1080/089419299279704.
- Hough, J.L., 1993. Why burn the bush? Social Approaches to Bush-Fire Management in West African National Parks, *Biological Conservation* 65, 23–28.
- Huffman, M.R., 2013. The many elements of traditional fire knowledge: Synthesis, classification, and aids to cross-cultural problem solving in fire-dependent systems around the world. *Ecol. Soc.* 18 <https://doi.org/10.5751/ES-05843-180403>.
- J. Muñoz Sabater, ERA5-Land hourly data from 1981 to present, <https://cds.climate.copernicus.eu/cdsapp!/dataset/10.24381/cds.e2161bac?tab=overview>, copernicus Climate Change Service (C3S) Climate Data Store (CDS). Accessed on 2023-01-16 (2019).
- Laris, P., 2002. Burning the Seasonal Mosaic: Preventative Burning Strategies in the Wooded Savanna of Southern Mali. *Hum. Ecol.* 30, 155–186.
- Lehmann, C.E.R., Archibald, S.A., Hoffmann, W.A., Bond, W.J., 2011. Deciphering the distribution of the savanna biome. *New Phytol.* 191, 197–209. <https://doi.org/10.1111/j.1469-8137.2011.03689.x>.
- M. P. Martín, I. Gómez, E. Chuvieco, Burnt area index (baim) for burned area discrimination at regional scale using modis data, *Forest Ecology and Management* 234 (2006) S221. doi:10.1016/j.foreco.2006.08.248.
- S. W. Maier, J. Russell-Smith, Measuring and monitoring of contemporary fire regimes in Australia using satellite remote sensing, in: *Flammable Australia : fire regimes, biodiversity and ecosystems in a changing world*, CSIRO, 2012, Ch. 4, pp. 79–96.
- J. Mistry A. Berardi V. Andrade T. Kraho P. Kraho O. Leonardos Indigenous fire management in the cerrado of Brazil: The case of the Kraho of Tocantins *Human Ecology* 33 2005 365 386 10.1007/s10745-005-4143-8.
- MODIS Collection 6 Hotspot / Active Fire Detections MCD14ML distributed from NASA FIRMS, <https://earthdata.nasa.gov/firms>, accessed: 2022-06-30. doi:10.5067/FIRMS/MODIS/MCD14ML.
- D. M. Olson, E. Dinerstein, E. D. Wikramanayake, N. D. Burgess, G. V. N. Powell, E. C. Underwood, J. A. D'Amico, I. Itoua, H. E. Strand, J. C. Morrison, C. J. Loucks, T. F.

- Allnutt, T. H. Rick- etts, Y. Kura, J. F. Lamoreux, W. W. Wettengel, P. Hedao, K. R. Kassem, Terrestrial Ecoregions of the World: A New Map of Life on Earth: A new global map of terrestrial ecoregions provides an innovative tool for conserving biodiversity, *BioScience* 51 (11) (2001) 933–938. arXiv:<https://academic.oup.com/bioscience/article-pdf/51/11/933/26890733/51-11-933.pdf>, doi:10.1641/0006-3568(2001)051[0933:TEOTWA]2.0.CO;2. URL [https://doi.org/10.1641/0006-3568\(2001\)051\[0933:TEOTWA\]2.0.CO;2](https://doi.org/10.1641/0006-3568(2001)051[0933:TEOTWA]2.0.CO;2).
- Perry, J.J., Cook, G.D., Graham, E., Meyer, C.P., Murphy, H.T., Vanderwal, J., 2019. Regional seasonality of fire size and fire weather conditions across Australia's northern savanna. *Int. J. Wildland Fire* 29, 1–10. <https://doi.org/10.1071/WF19031>.
- Perry, J.J., Cook, G.D., Graham, E., Meyer, C.P., Murphy, H.T., Vanderwal, J., 2020. Regional seasonality of fire size and fire weather conditions across Australia's northern savanna. *International Journal of Wildland Fire* 29, 1–10. <https://doi.org/10.1071/WF19031>.
- V.R. Pivello The use of fire in the cerrado and Amazonian rainforests of Brazil: Past and present, *Fire Ecology* 7 2011 24 39 10.4996/fireecology.0701024.
- Price, O.F., Russell-Smith, J., Watt, F., 2012. The influence of prescribed fire on the extent of wildfire in savanna landscapes of western Arnhem Land, Australia, *International Journal of Wildland Fire* 21, 297. <https://doi.org/10.1071/WF10079>.
- R. Ramo, E. Roteta, I. Bistinas, D. van Wees, A. Bastarrika, E. Chuvieco, G. R. van der Werf, African burned area and fire carbon emissions are strongly impacted by small fires undetected by coarse resolution satellite data, *Proceedings of the National Academy of Sciences of the United States of America* 118 (3 2021). doi:10.1073/pnas.2011160118.
- Rissi, M.N., Baeza, M.J., Gorgone-Barbosa, E., Zupo, T., Fidelis, A., 2017. Does season affect fire behaviour in the Cerrado? *Int. J. Wildland Fire* 26, 427–433. <https://doi.org/10.1071/WF14210>.
- J. Russell-Smith C. Monagle M. Jacobsohn R.L. Beatty B. Bilbao A. Millan, H. Vessuri, I. Sanchez-Rose, Can savanna burning projects deliver measurable greenhouse emissions reductions and sustainable livelihood opportunities in fire-prone settings? *Climatic Change* 140 2013 47 61 10.1007/s10584-013-0910-5. doi: 10.1007/s10584-013-0910-5.
- Russell-Smith, J., Yates, C., Edwards, A., Allan, G.E., Cook, G.D., Cooke, P., Craig, R., Heath, B., Smith, R., 2003. Contemporary fire regimes of northern Australia, 1997–2001: change since Aboriginal occupancy, challenges for sustainable management. *International Journal of Wild- Land Fire* 12, 283. <https://doi.org/10.1071/WF03015>.
- Russell-Smith, J., Yates, C., Vernooij, R., Eames, T., van der Werf, G., Ribeiro, N., Edwards, A., Beatty, R., Lekoko, O., Mafoko, J., Monagle, C., Johnston, S., 2021. Opportunities and challenges for savanna burning emissions abatement in southern Africa. *J. Environ. Manage.* 288 <https://doi.org/10.1016/j.jenvman.2021.112414>.
- I. Sackey, W. Hale, Effects of Perennial Fires on the Woody Vegetation of Mole National Park, Ghana, *Journal of Science and Technology (Ghana)* 28 (9 2008). doi:10.4314/just.v28i2.33092.
- Sankaran, M., Hanan, N.P., Scholes, R.J., Ratnam, J., Augustine, D.J., Cade, B.S., Gignoux, J., Higgins, S.L., Roux, X.L., Ludwig, F., Ardo, J., Banyikwa, F., Bronn, A., Bucini, G., Caylor, K.K., Coughenour, M.B., Diouf, A., Ekaya, W., Feral, C.J., February, E.C., Frost, P.G., Hiernaux, P., Hrabar, H., Metzger, K.L., Prins, H.H., Ringrose, S., Sea, W., Tews, J., Worden, J., Zambatis, N., 2005. Determinants of woody cover in African savannas. *Nature* 438, 846–849. <https://doi.org/10.1038/nature04070>.
- Scholes, R.J., Archer, S.R., 1997. Tree-Grass Interactions in Savannas, *Source. Annu. Rev. Ecol. Syst.* 28, 517–561.
- Scholes, R., Walker, B., 1993. *An African savanna : synthesis of the Nylsvley study.* Cambridge University Press.
- Simon, M.F., Pennington, T., 2012. Evidence for adaptation to fire regimes in the tropical savannas of the Brazilian Cerrado. *Int. J. Plant Sci.* 173, 711–723. <https://doi.org/10.1086/665973>.
- U. E. P. (UNEP), I. U. for Conservation of Nature (IUCN), World Database on Protected Areas, <https://www.protectedplanet.net/en/thematic-areas/wdpa?tab=WDPA>, accessed on 2023-01-15.
- G.R.V.D. Werf J.T. Randerson L. Giglio T.T.V. Leeuwen Y. Chen B.M. Rogers M. Mu M.J. V. Marle D.C. Morton G.J. Collatz R.J. Yokelson P.S. Kasibhatla Global fire emissions estimates during 1997–2016 *Earth System Science Data* 9 2017 697 720 10.5194/essd-9-697-2017.
- Williams, R.J., Gill, A.M., Moore, P.H.R., 2003. *Fire in Tropical Savannas: the Kapalga Experiment*, Springer-Verlag: New York. Ch. 3, 33–46.
- M. J. Wooster, G. J. Roberts, L. Giglio, D. Roy, P. Freeborn, L. Boschetti, C. Justice, C. Ichoku, W. Schroeder, D. Davies, A. Smith, A. Setzer, I. Csizsar, T. Strydom, P. Frost, T. Zhang, W. Xu, M. de Jong, J. Johnston, L. Ellison, K. Vadrevu, J. McCarty, V. Tanpipat, C. Schmidt, J. San-Miguel, Satellite remote sensing of active fires: History and current status, applications and future requirements (12 2021). doi:10.1016/j.rse.2021.112694.